Astronomy Reports, Vol. 45, No. 7, 2001, pp. 569–576. Translated from Astronomicheskiĭ Zhurnal, Vol. 78, No. 7, 2001, pp. 661–668.

Convective Mechanism for the Formation of Photospheric Magnetic Fields

A. V. Getling

Institute of Nuclear Physics, Lomonosov Moscow State University, Moscow, 117234 Russia
e-mail: A.Getling@ru.net

Received October 16, 2000

Abstract—The well-known model that attributes the formation of a bipolar sunspot group to the emergence of a flux tube disagrees sharply with the usual observed pattern of phenomena. At the same time, the observed patterns can be accounted for quite convincingly in terms of local magnetic-field amplification due to cellular convective motions of the solar plasma. In this study, magnetoconvection in a plane horizontal fluid layer is simulated numerically in the framework of the fully nonlinear, three-dimensional problem. A weak horizontal magnetic field and weak cellular flow are assumed to be present initially. Convection is shown to be capable of producing bipolar magnetic configurations of the strongly amplified magnetic field. Indications of magnetic freezing of the flow in the cell are found. The action of the amplification mechanism under study may be controlled by the large-scale toroidal magnetic field of the Sun. *© 2001 MAIK "Nauka/Interperiodica".*

1. INTRODUCTION

The traditional scheme describing the formation of the magnetic field of a bipolar sunspot group (often silently assumed to be virtually unquestionable) is based on the idea that a magnetic flux tube lies at some depth below the solar photosphere. The strength of the magnetic field in the tube locally reaches a value sufficient for the tube to emerge under the action of magnetic buoyancy. The segment of the tube that has emerged intersects the photosphere at two sites, and two spots of opposite magnetic polarities arise precisely at these sites [1]. This view can also account for some global regularities in solar activity, e.g., the Hale law.

However, the rising-tube model can hardly offer an adequate representation of reality. First, if it is adopted, one has to account for the origin of the strong magnetic field in the tube; to this end, some additional, fairly artificial assumptions need to be introduced. Second, and especially important, is that the evolution pattern inferred from this model for a local photospheric magnetic field disagrees sharply with the corresponding pattern actually observed on the Sun. Let us list the main points of this disagreement.

(1) The strong magnetic field present in the tube would affect the convective flow even before the emergence of the tube on the surface, and subsequently the rising tube would completely break down the existing supergranular velocity field. In contrast, the actually observed flow patterns normally remain almost invariable in the process of local magnetic-field amplification [2].

(2) Certain dramatic effects, such as plasma streams spreading from the site above the rising tube, should be especially impressive but have never been observed.

(3) The emerging magnetic field itself, strong and mainly horizontal, would be directly observed in the photosphere as one of the most prominent features of the process. Nothing of the sort actually takes place.

(4) The emergence of a tube implies a sharp discrepancy in direction between the streamlines and magnetic field lines. In reality, as a spot develops, the magnetic field gradually *seeps* through the photosphere without disrupting the existing velocity field [2].

(5) According to the observations of Bumba [2], the area distribution of sunspots exhibits pronounced peaks near multiples of the area of a supergranule. Such spot-area quantization cannot be accounted for in the rising-tube model.

At the same time, an alternative possibility was suggested 35 years ago by Tverskoy [3]. He associated the process of local magnetic-field amplification with the actually observed convective motions of the solar matter in supergranules. The solar plasma circulating in a supergranular cell can amplify the magnetic field to high strengths and form a bipolar magnetic configuration typical of a sunspot group. Tverskoy's hypothesis naturally and easily overcomes the serious difficulties encountered by the rising-tube model. At the same time, the mechanism suggested by Tverskoy fits into the overall picture of solar activity at least as well as the tube mechanism does.

Tverskoy considered a simple kinematic model, assuming the fluid motion to be predefined and independent of the magnetic field. The velocity field in the supergranular convection cell was approximated by a toroidal eddy, and the electrical conductivity of the fluid was assumed to be infinite. A weak horizontal magnetic field was specified at the initial time. The

1063-7729/01/4507-0569$21.00 © 2001 MAIK "Nauka/Interperiodica"

"winding" of magnetic field lines by the eddy produced two bunches of lines of amplified field, opposite in polarity and situated in diametrically opposed parts of the vortex ring—a bipolar magnetic configuration. This approach made it possible to arrive at a number of generalizations [4, 5]. In addition, it demonstrated the possibility of the action of a global solar hydromagnetic dynamo based on the idea of an ensemble of toroidal eddies (cells) with an azimuthal (Coriolis) velocity component, distributed over the entire convective envelope of the Sun [6].

If we suppose that precisely this convective mechanism is responsible for the formation of the bipolar magnetic configurations observed on the Sun, any artificial assumptions concerning the advance formation of flux tubes of strong magnetic fields become unnecessary, and the predicted picture comes into agreement with observations. The magnetic field lines will be stretched along streamlines, and the magnetic flux will gradually percolate through the solar surface.

However, the kinematic model leaves many questions unresolved. Among them is the most important issue of the efficiency of the mechanism under study: Can a real convection cell provide sufficient magnetic-field amplification before the flow in this cell is slowed down or the cell is disrupted by instabilities?

The convective amplification of a magnetic field is a strongly nonlinear and fundamentally three-dimensional mechanism. A thorough analysis and deep substantiation of the convective mechanism for the formation of photospheric magnetic fields thus require numerical simulations of the evolution of three-dimensional flows and magnetic fields based on a full system of magnetohydrodynamic equations. High spatial resolution is necessary for the computational scheme; such calculations have become possible only in recent years.

Some results obtained in this way will be presented here. At this early stage of investigation, we will restrict ourselves to the Boussinesq approximation (see, e.g., [7]). In other words, we will assume density variations to be negligibly small in all terms of the equations except for the term proportional to the gravitational acceleration.

Let us note that, although numerical simulations of three-dimensional magnetoconvection have been carried out for a relatively long time by various groups around the world, the mechanism of magnetic-field amplification and structuring has not been comprehensively studied. Most frequently, studies have been concerned with the effect (discovered by Weiss [8]) of spatial separation of the flow and the magnetic flux, which arises as the convection interacts with an initially imposed—as a rule, vertical—magnetic field ([9] is noteworthy among the most recent investigations in this cycle); some studies have focused attention on the oscillation and wave processes inherent in compressible magnetoconvection (as, e.g., in [10]).

2. FORMULATION OF THE PROBLEM OF NONLINEAR NUMERICAL SIMULATION

We will solve the system of magnetohydrodynamic equations in the Boussinesq approximation for a plane horizontal layer $0 < z < d$ of a fluid with finite electrical conductivity heated from below. Imagine that the layer under study is bounded from below and above by slabs of a motionless material, perfectly electrically and thermally conductive, and that the lower and upper boundary are kept at constant temperatures T_1 and T_2, respectively, their difference being ΔT. We represent any variable f of the problem as the sum of its *unperturbed* value f_0, which corresponds to the motionless state of the fluid, and a *perturbation*, which is produced by the flow (and, in general, can even substantially exceed the unperturbed value). We take the unperturbed (initial) magnetic field $\mathbf{H}_0$ to be uniform and directed horizontally, along the x axis. We denote the magnetic-field perturbation, measured in units of H_0, as $\mathbf{h}$. The perturbation of the temperature—i.e., its departure from the equilibrium, linear profile $T_0 = T_1 - \Delta T(z/d)$, expressed in units of ΔT—will be designated as θ. We choose d as the unit length and the characteristic time $t_\nu = d^2/\nu$ for viscous dissipation on the scale d as the unit time (here, ν is the kinematic viscosity). We denote the dimensionless velocity as $\mathbf{u}$.

Let us write the original system of equations in the following dimensionless form:

$$\frac{\partial \mathbf{u}}{\partial t} + (\mathbf{u}\nabla)\mathbf{u} = -\nabla\varpi + \frac{R}{P_1}\hat{\mathbf{z}}\theta - \frac{Q}{P_2}([\hat{\mathbf{H}}_0 \operatorname{curl}\mathbf{h}] + [\mathbf{h}\operatorname{curl}\mathbf{h}]) + \Delta\mathbf{u}, \tag{1}$$

$$\frac{\partial \mathbf{h}}{\partial t} = \operatorname{curl}[\mathbf{u}\hat{\mathbf{H}}_0] + \operatorname{curl}[\mathbf{u}\mathbf{h}] + \frac{1}{P_2}\Delta\mathbf{h}, \tag{2}$$

$$\frac{\partial \theta}{\partial t} - u_z + (\mathbf{u}\nabla)\theta = \frac{1}{P_1}\Delta\theta, \tag{3}$$

$$\operatorname{div}\mathbf{u} = 0, \tag{4}$$

$$\operatorname{div}\mathbf{h} = 0. \tag{5}$$

Here, $\hat{\mathbf{H}}_0 = \mathbf{H}_0/H_0$, and $\hat{\mathbf{z}}$ is a unit vector directed along the z coordinate axis, vertically upward. The quantity ϖ is the dimensionless form of the combination p'/ρ_0 (where p' is the pressure perturbation and ρ_0 is the density at temperature T_0). The dimensionless parameters

$$R = \frac{\alpha g \Delta T d^3}{\nu\chi}, \quad Q = \frac{H_0^2 d^2}{4\pi\rho_0\nu\nu_m} = \frac{H_0^2 d^2 \sigma}{\rho_0 c^2 \nu}, \quad P_1 = \frac{\nu}{\chi}, \quad P_2 = \frac{\nu}{\nu_m} = \frac{4\pi\sigma\nu}{c^2} \tag{6}$$

(where α is the volumetric thermal-expansion coefficient of the fluid, χ its thermal diffusivity, σ its electri-

cal conductivity, and ν_m its magnetic viscosity) are the Rayleigh number, Chandrasekhar number, normal Prandtl number, and magnetic Prandtl number, respectively.

We assume the surfaces of the layer to be free-slip and impermeable; i.e., we specify the condition that the normal (vertical) velocity component and tangential stresses vanish at these surfaces:

$$u_z = \frac{\partial u_x}{\partial z} = \frac{\partial u_y}{\partial z} = 0 \quad \text{at} \quad z = 0, 1. \tag{7}$$

If the slabs bounding the layer are perfectly electrically conducting, the boundary conditions for the magnetic field have a quite similar form:

$$h_z = \frac{\partial h_x}{\partial z} = \frac{\partial h_y}{\partial z} = 0 \quad \text{at} \quad z = 0, 1. \tag{8}$$

In this formulation of the problem, the temperature perturbations vanish at the layer boundaries:

$$\theta = 0 \quad \text{at} \quad z = 0, 1. \tag{9}$$

We employ the Galerkin method in the form described by Orszag [11]. We assume the velocity field, magnetic field, and thermal-perturbation field to be periodic functions of the coordinates x and y. We introduce spectral representations of these functions in the form of partial sums of trigonometric Fourier series; the boundary conditions (7)–(9) also make it possible to choose trigonometric functions to describe the z dependences. The full wavevector of a harmonic with numbers l, m, n will be $\mathbf{k}_{lmn} = \{l\alpha, m\beta, n\pi\}$, with $l < K_x$, $m < K_y$, $n < K_z$; here, α and β are the wavenumbers specifying the fundamental periods in x and y, respectively, and K_x, K_y, K_z are the spectrum bounds chosen for the computations. To reduce the number of variables, we restrict our consideration to physical fields with a certain symmetry with respect to the coordinate origin (see Figs. 1, 2, 4 below); in this case, the spectral coefficients (harmonic amplitudes) will obey certain parity relations in l and m.

Substitution of the spectral representations into the original system (1)–(5) reduces it to a system of ordinary differential equations for the harmonic amplitudes as functions of time. Following Orszag [11], we use a fast Fourier transformation to calculate the convolution sums in the right-hand sides of the spectral equations, and employ the fourth-order Runge–Kutta method to carry out the integration over time.

3. RESULTS

All the computation runs whose results are presented here were conducted for $K_x = K_y = K_z = 32$ (the run simulating a nonmagnetic flow, which assumes $K_x = K_y = K_z = 16$, is an exception). By virtue of the symmetry chosen for the initial perturbation, the number of harmonics representing the dependence of the physical fields on any coordinate is 32; therefore, the total number of basis functions used in the Galerkin representation is $32^3 = 32768$ for each variable.

In each run, a weak perturbation of the motionless state of the fluid was specified at the initial time, in the form of a collection of Bénard-type hexagonal cells (Fig. 1a); viz.,

$$u_z = -4\frac{A}{\pi}(2\cos\sqrt{3}\beta x\cos\beta y + \cos 2\beta y)\cos\pi z \quad \text{at} \quad t = 0, \tag{10}$$

where $A = -0.1$, $\beta = 2$ [with the corresponding expressions for u_x and u_y according to (4)].

We first consider the evolution of the velocity field in the absence of a magnetic field ($Q = 0$, Fig. 1); qualitatively, this pattern of evolution also holds in a number of MHD scenarios. For the conditions chosen, the three-dimensional convection regime is metastable. Fairly soon, before $t = 1$, a steady cellular flow is established (Fig. 1b); at that time, in the midplane $z = 1/2$ of the layer, the maximum value of u_z (at the center of the cell) exceeds the minimum value (at the vertices of the hexagon) in absolute magnitude. This regime is observed until at least $t = 9$. Further, the hexagonal cells undergo a sudden breakdown, and a transition to a two-dimensional roll flow takes place (Figs. 1c, 1d); in this flow, the minimum and maximum velocities over the horizontal cross section of the cell are equal in absolute magnitude (this complete history of the temporal variations of $\max u_z$ and $\min u_z$ is also observed in most scenarios with a magnetic field; see Figs. 3a and 3b below).

For the initial conditions considered, the rolls that ultimately arise from hexagons are oriented along the x axis and can be represented to first approximation by the function

$$u_z = B\cos\beta y. \tag{11}$$

It is clear that, in the case at hand, the rows of central upwellings situated in the system of hexagonal cells along different straight lines $y = \text{const}$ (e.g., $y = 0$ and $y = \pm 1.57$ in Fig. 1b) cannot behave similarly, since some rows change into continuous upflow zones, while others change into downflow zones. In the direction of the y axis, rows in which the upwellings merge (e.g., along the lines $y = \pm 1.57$) alternate with rows where the upwellings are compressed (at $y = 0$) and then disappear, giving way to expanding downflows (Figs. 1c, 1d). In which specific rows (even or odd ones, when counted along the y axis) the upwellings will merge depends on uncontrolled noise perturbations.

Note that the flow pattern of two-dimensional rolls, typical of convection in horizontal fluid layers weakly nonuniform in the vertical direction, should not necessarily arise in the solar convection zone, where compressibility and other factors complicating the stratification are present. Without discussing possibilities for

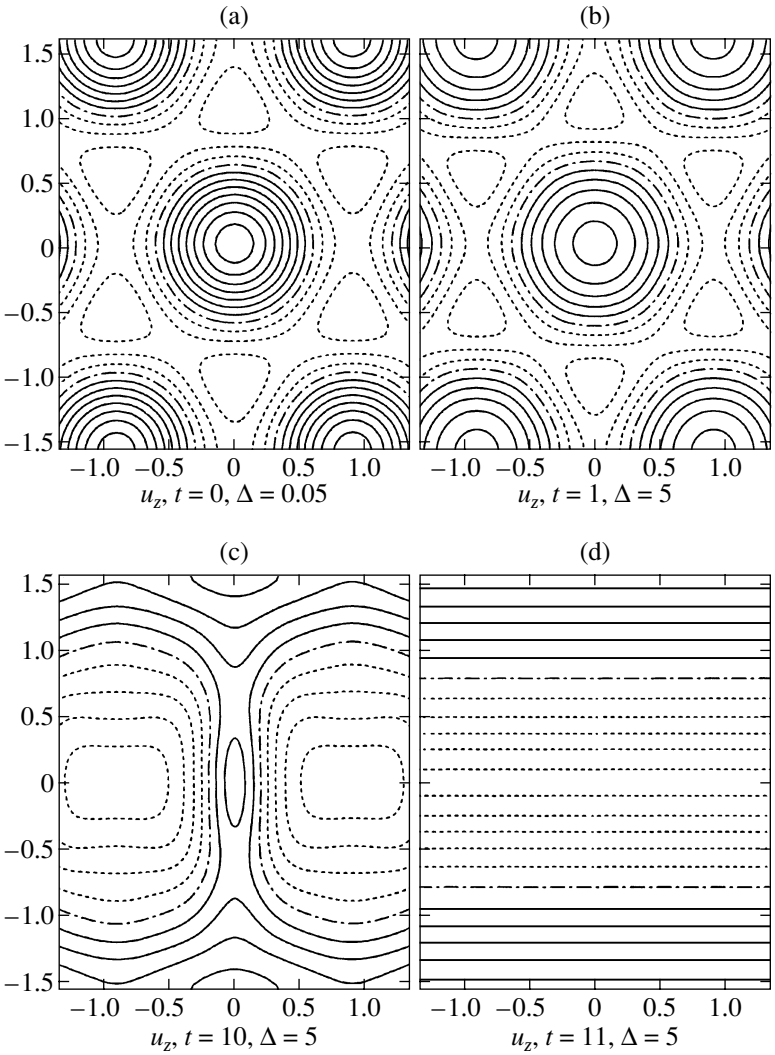

Fig. 1. Evolution of the flow in the absence of a magnetic field for $R = 3000 = 4.56R_c$ and $P_1 = 1$. Contours of the vertical velocity component u_z in the midplane $z = 1/2$ of the layer are shown with contour increment Δ (here, as in Figs. 2 and 4 below, the solid lines correspond to positive values, the dash–dot lines to zero, and dashed lines to negative values): (a) initial perturbation; (b) well-established cellular flow; (c) transition from the cellular to a roll flow; and (d) well-established roll flow.

two-dimensional convection on the Sun, we will be interested here only in phenomena occurring at the stage when the flow is three-dimensional.

We now consider the evolution of the flow and magnetic field for $R = 3000 = 4.56R_c$, $Q = 0.01$, $P_1 = 1$, and $P_2 = 10$ (Figs. 2, 3a; here, $R_c = 657.5$ is the critical Rayleigh number at which convection sets in). Crudely, by the time $t = 0.5$, the cellular flow settles down to a steady state, which persists almost until $t = 9$. During the interval $0 < t < 2$, the magnetic field is amplified by the flow, and characteristically bipolar configurations—pairs of compact magnetic islands—develop in the zones of convective upwelling, near the cell centers. At $t = 2$ or so, they reach a steady state, with a magnetic-field strength of about 41.5 (in units of H_0) within the islands. The magnetic islands remain nearly identical in all upwellings as long as the velocity field retains its original symmetry.

After $t \approx 9.5$, a rapid transition to a two-dimensional roll flow takes place. The magnetic field weakens in merging upwellings (in the case under consideration, e.g., along the line $x = 0$) and, on the contrary, is additionally amplified for some time in those upwellings that undergo compression ($x = \pm 1.57$); this is reflected by the peak in the curve of $\max H_z$ in Fig. 3a near $t = 9.9$, whose height is 49.1. Ultimately, the component of the magnetic field produced by convection decays, and the fields returns to its initial state. As is well known [12], an externally imposed horizontal magnetic field favors the formation of rolls oriented along this field. Such rolls cannot amplify the magnetic field. Nevertheless, in our case, the fairly weak initial field does not inhibit

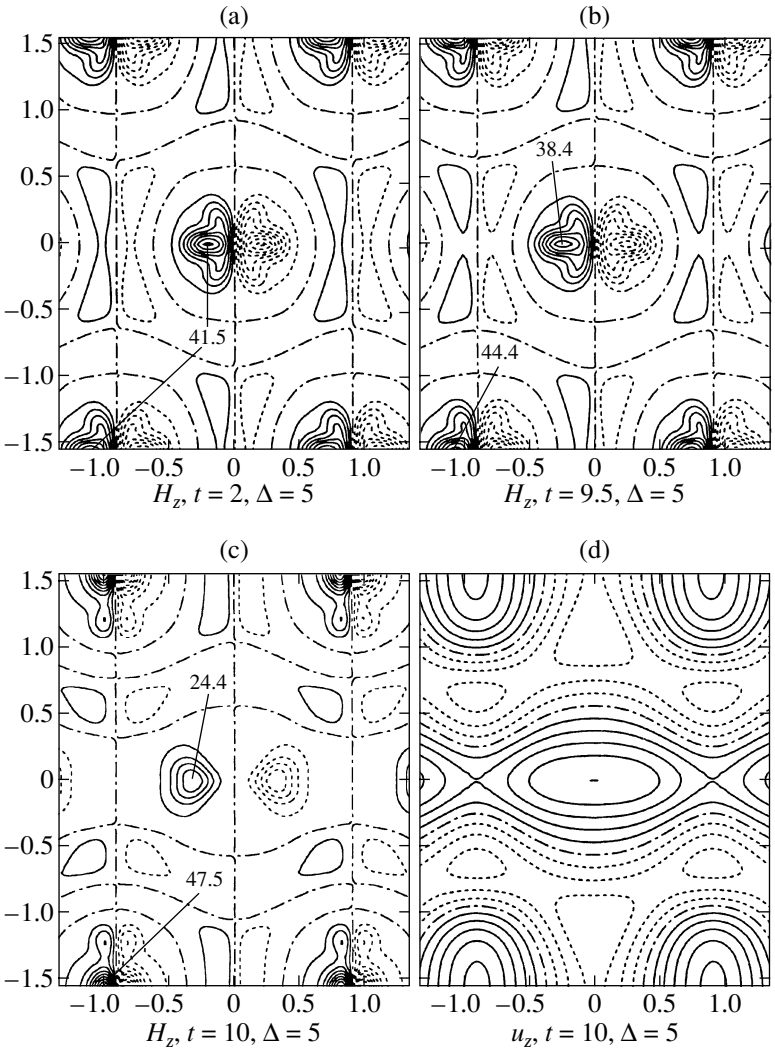

Fig. 2. Evolution of the flow and magnetic field for $R = 3000 = 4.56R_c$, $P_1 = 1$, $P_2 = 10$, and $Q = 0.01$. Contours of the vertical components of the magnetic field H_z and velocity u_z in the midplane $z = 1/2$ of the layer are shown with contour increment Δ: (a) well-established distribution of H_z; (b) deformation of the distribution of H_z shortly after the loss of the steady state and cell symmetry; and (c, d) distributions of H_z and u_z, respectively, at the stage of the transition from the cellular flow to a roll flow. Same notation as in Fig. 1 is used for the contours.

the development of three-dimensional convective flows.

Varying the Chandrasekhar number Q (actually, the initial magnetic-field strength) with other parameters fixed demonstrates that the main features of the scenario described are typical of the range $0.001 < Q < 1$ studied (the cases of $Q = 0.001$ and $Q = 0.01$ are very similar not only qualitatively, but also quantitatively). A comparison of scenarios computed for various Q values (Fig. 3) shows that a strong initial field ($Q = 1$) results in a rapid transition to rolls, while the period of existence of the three-dimensional flow becomes longer as Q is decreased.

The influence of the parameters R and P_2 can easily be predicted. An increase in the Rayleigh number R to $4000 = 6.08R_c$ raises the steady-state value of $\max H_z$ to 49.2 and the peak value (at $t \approx 7.6$) to 50.9. The efficiency of magnetic-field amplification grows rapidly with increase of the magnetic Prandtl number P_2. For $P_2 = 30$, as can be seen from Fig. 4, the value of $\max H_z$ at the steady-state stage proves to be much larger than for $P_2 = 10$, and even exceeds 170 at the upwelling-compression stage. The islands of amplified magnetic field at $P_2 = 30$ are more compact than at $P_2 = 10$.

4. DISCUSSION

Thus, our computations confirm qualitative conclusions based on the model of Tverskoy [3]. In any particular case, the efficiency of the convective mechanism

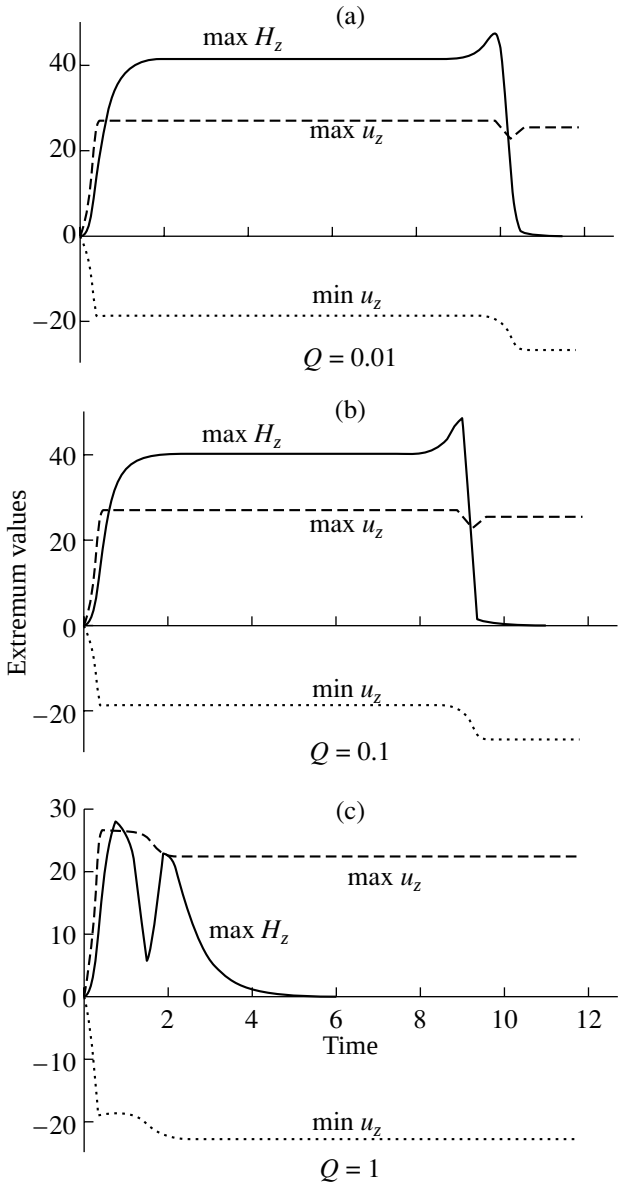

Fig. 3. Time variation of extremum values of the vertical components of the magnetic field and velocity for $R = 3000 = 4.56R_c$, $P_1 = 1$, $P_2 = 10$, and (a) $Q = 0.01$, (b) $Q = 0.1$, and (c) $Q = 1$.

can be measured by the maximum achieved dimensionless H and the ratio γ of the maximum values of the magnetic- and kinetic-energy densities E_m and E_k:

$$E_m = \frac{H_0^2(\max H_z)^2}{8\pi}, \quad E_k = \frac{\rho_0(\max u_z)^2}{2}\frac{\nu^2}{d^2}, \qquad \gamma = \frac{E_m}{E_k} = \frac{Q(\max H_z)^2}{P_2(\max u_z)^2}. \tag{12}$$

This ratio increases with R and P_2, and also with Q—until the flow braking by the magnetic field becomes strong. In particular, in the scenarios presented in Fig. 3, $\gamma \approx 0.003$ for $Q = 0.01$ (Fig. 3a), $\gamma \approx 0.032$ for $Q = 0.1$ (Fig. 3b), and $\gamma \approx 0.1$ for $Q = 1$ (Fig. 3c); in the last case, the braking is fairly strong, and the amplified magnetic field rapidly disrupts the three-dimensional flow. In the case illustrated by Fig. 4, $\gamma \approx 0.013$, while the preliminary results obtained for $R = 5000$, $P_1 = 1$, $P_2 = 30$ yield $\gamma \approx 1$ for $Q = 1$ and $\gamma \approx 1.24$ for $Q = 3$. Since a 170-fold amplification is possible at quite moderate values of R and P_2, larger values of these parameters could undoubtedly provide amplification by factors of many hundreds or even thousands. Thus, the convective magnetic-field amplification mechanism described here should be very efficient and is promising in the context of searches for sources of strong photospheric magnetic fields. In particular, our computations demonstrate the possibility of the formation of very compact magnetic islands. For this reason, it will be useful to investigate the possible role of this mechanism in producing not only sunspots and active regions, but also compact magnetic elements.

A comparison between the computation runs with and without a magnetic field shows that the amplified magnetic field can leave the flow structure and velocity in a cell virtually unaffected. This is likely a manifestation of the effect predicted earlier from the kinematic model [13]. The Ampére force of flow braking due to the magnetic field is determined by the product $[\mathbf{H}\mathrm{curl}\mathbf{H}] \cdot \mathbf{v}$. The $\mathbf{H}$ component that grows with time is parallel to the velocity vector $\mathbf{v}$, whereas the component normal to $\mathbf{v}$ is of the order of the initial field $\mathbf{H}_0$. Therefore, the braking force is proportional to $H_0|\mathrm{curl}\mathbf{H}|$. Given the order of magnitude of the amplified field $\mathbf{H}$, the energy losses due to braking will be smaller the weaker the initial field $\mathbf{H}_0$. One can easily imagine situations where larger final amplified field strengths will be achieved with smaller initial field strengths—of course, if the flow in the cell remains stable, and the process develops in accordance with the model scenario.

Moreover, the amplified field aligned with the streamlines should stabilize the fluid flow. The lines of the amplified field are "rails" laid by the flow, which should counteract changes in the flow configuration. At the same time, the magnetic-field component normal to the velocity vector, which can destabilize the flow, retains a magnitude of order H_0. Thus, weak magnetic fields are favorable for the operation of this mechanism also in terms of stability. It is possible that, at sufficiently small H_0 and sufficiently large magnitude of the amplified magnetic field, the latter will exert a "freezing" effect on the flow.

At this stage, it would be premature to attempt to estimate the parameter values typical of the solar convection zone, where the viscosity and thermal conductivity are controlled by turbulent transport and are thus highly indeterminate. Large Rayleigh numbers R can be expected; however, the mere presence of a relatively regular supergranular pattern on the Sun suggests that

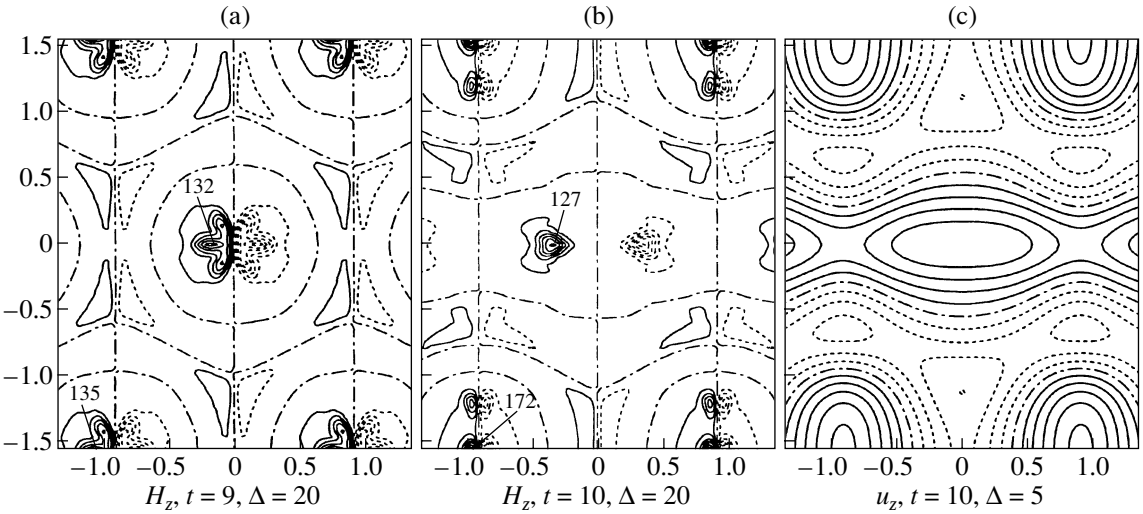

Fig. 4. Evolution of the flow and magnetic field for $R = 3000 = 4.56R_c$, $P_1 = 1$, $P_2 = 30$, and $Q = 0.01$. Contours of the vertical components of the magnetic field H_z and velocity u_z in the midplane $z = 1/2$ of the layer are shown with contour increment Δ: (a) deformation of the distribution of H_z shortly after the loss of the steady state and cell symmetry; (b, c) distributions of H_z and u_z, respectively, at the stage of the transition from the cellular flow to a roll flow. Same notation as in Fig. 1 is used for contours.

the effective R for the corresponding layers is maintained by small-scale turbulent processes on a level at which convection remains quasi-laminar. The electrical conductivity of the solar plasma in the convection zone grows rapidly with depth, reaching values for which the magnetic field can be considered to be completely frozen in the plasma. Turbulence should reduce the effective conductivity. However, as can be judged by the observed picture, the magnetic-field dynamics do not depart too strongly from a freezing-in regime, even in layers that can be directly observed; therefore, the magnetic Prandtl number P_2 still remains fairly high. Effective hydrodynamic Prandtl numbers of order unity are usually considered plausible.

The pattern of the evolution of photospheric magnetic fields controlled by the convective mechanism is free of the contradictions with observations inherent in the rising-tube model (see Introduction).

For the convective mechanism to come into action, it is necessary that an especially large and intense supergranular cell encompassing layers deeper than usual be threaded with a weak seed magnetic field. Such a field is unlikely to be highly ordered, but the spatially averaged vector of this field could naturally be identified with the large-scale toroidal (latitudinally directed) magnetic field; the presence of such a preferred direction of the magnetic field at the initial time is, in principle, sufficient for the field to subsequently evolve in qualitative agreement with the computed scenarios. Therefore, the seed field should be controlled by large-scale dynamo processes, and should introduce a global regularity into the distribution of sunspot groups. Nothing but convection on supergranular and sunspot scales will serve as a connecting link between the global and local processes.

Diverse initial conditions can ensure the generation of diverse configurations of the amplified magnetic field. In particular, if the initial magnetic field is directed vertically, a unipolar-type configuration will form, whereas oblique initial fields will produce a variety of superpositions of unipolar, bipolar, and higher multipolar fields. If the seed field threads a group of cells, the interaction of the flows with the magnetic field will be "collective," and the amplified field will have a more complex structure; in this case, natural prerequisites arise for the manifestation of the sunspot-area quantization pointed out in [2].

Let us summarize the main conclusions of this study.

(1) The convective mechanism considered here, which does not require strong initial magnetic fields, is highly efficient, i.e., it can form bipolar configurations of a multiply amplified magnetic field.

(2) This mechanism provides a natural explanation for the general, global regularities in the behavior of local solar magnetic fields and for the quantization of sunspot areas.

(3) The basic features of the magnetic-field amplification process are in agreement with the observed pattern for the evolution of flows and magnetic fields in the regions where sunspot groups develop.

5. ACKNOWLEDGMENTS

I am grateful to the Pushchino Radio Astronomy Observatory of the Russian Academy of Sciences for computer-resource allocation, to I.L. Ovchinnikov for invaluable help in arranging and performing the computations, and to L.M. Alekseeva for perpetual fruitful discussions. This work was supported by the Russian Foundation for Basic Research (project code 00-02-16313).

REFERENCES

1. E. N. Parker, Astrophys. J. **121**, 491 (1955).
2. V. Bumba, *Rendiconti della Scuola Internazionale di Fisica* "*E.Fermi*," 39 Corso (1967), p. 77.
3. B. A. Tverskoy, Geomagn. Aeron. **6** (1), 11 (1966).
4. A. V. Getling and B. A. Tverskoy, Astron. Zh. **45** (3), 606 (1968).
5. A. V. Getling, Dokl. Akad Nauk SSSR **187** (2), 301 (1969).
6. A. V. Getling and B. A. Tverskoy, Geomagn. Aeron. **11** (2), 211 (1971); **11** (3), 389 (1971).
7. A. V. Getling, *Rayleigh–Bénard Convection: Structures and Dynamics* (World Scientific, Singapore, 1998; URSS, Moscow, 1999).
8. N. O. Weiss, Mon. Not. R. Astron. Soc. **128**, 225 (1964).
9. L. Tao, N. O. Weiss, D. P. Brownjohn, and M. R. E. Proctor, Astrophys. J. Lett. **496**, L39 (1998).
10. N. E. Hurlburt, P. C. Matthews, and M. R. E. Proctor, Astrophys. J. **457** (2), 933 (1996).
11. S. A. Orszag, Stud. Appl. Math. **50** (4), 293 (1971); J. Fluid Mech. **49** (1), 75 (1971).
12. S. Chandrasekhar, *Hydrodynamic and Hydromagnetic Stability* (Oxford, Clarendon, 1961).
13. A. V. Getling, Astron. Zh. **45** (6), 1222 (1968).

Translated by A. Getling